CHALMERS
UNIVERSITY OF TECHNOLOGY

A Personalized Human Drivers' Risk Sensitive Characteristics Depicting Stochastic Optimal Control Algorithm for Adaptive Cruise Control

Citation for the original published paper (version of record):
Jiang, J., Ding, F., Zhou, Y. et al (2020). A Personalized Human Drivers' Risk Sensitive Characteristics Depicting Stochastic Optimal
Control Algorithm for Adaptive Cruise Control. IEEE Access, 8: 145056-145066.
http://dx.doi.org/10.1109/ACCESS.2020.3015349

IEEE Access
Multidisciplinary | Rapid Review | Open Access Journal

Received July 25, 2020, accepted August 2, 2020, date of publication August 10, 2020, date of current version August 19, 2020.

Digital Object Identifier 10.1109/ACCESS.2020.3015349

A Personalized Human Drivers' Risk Sensitive Characteristics Depicting Stochastic Optimal Control Algorithm for Adaptive Cruise Control

JIWAN JIANG[1,2], FAN DING[1], YANG ZHOU[2], JIAMING WU[3], AND HUACHUN TAN[1], (Member, IEEE)

[1]School of Transportation, Southeast University, Nanjing 211189, China
[2]Department of Civil and Environmental Engineering, University of Wisconsin–Madison, Madison, WI 53706, USA
[3]Department of Electrical Engineering, Chalmers University of Technology, SE-412 96 Gothenburg, Sweden

Corresponding authors: Fan Ding (fding5@seu.edu.cn) and Huachun Tan (tanhc@seu.edu.cn)

This work was supported by the National Key Research and Development Program of China under Grant 2019YFB1600100.

ABSTRACT This paper presents a personalized stochastic optimal adaptive cruise control (ACC) algorithm for automated vehicles (AVs) incorporating human drivers' risk-sensitivity under system and measurement uncertainties. The proposed controller is designed as a linear exponential-of-quadratic Gaussian (LEQG) problem, which utilizes the stochastic optimal control mechanism to feedback the deviation from the design car-following target. With the risk-sensitive parameter embedded in LEQG, the proposed method has the capability to characterize risk preference heterogeneity of each AV against uncertainties according to each human drivers' preference. Further, the established control theory can achieve both expensive control mode and non-expensive control mode via changing the weighting matrix of the cost function in LEQG to reveal different treatments on input. Simulation tests validate the proposed approach can characterize different driving behaviors and its effectiveness in terms of reducing the deviation from equilibrium state. The ability to produce different trajectories and generate smooth control of the proposed algorithm is also verified.

INDEX TERMS Adaptive cruise control, driving sensitive characteristic, expensive control, linear exponential-of-quadratic Gaussian, stochastic optimal control algorithm.

I. INTRODUCTION

Automated vehicles have drawn considerable attention widespread from the public recently since they have been expected to have a transformative impact on road transportation, for instance, to address critical traffic issues such as energy and capacity shortage. AVs are those equipped with embedded sensors named on-board units (OBUs) such as Radar or LIDAR to acquire real-time driving information from the leading vehicle via the detecting process [1], [2]. Among vehicle automation functions, longitudinal control, such as adaptive cruise control plays an essential role to automatically adjust their speeds to maintain a desired distance from the preceding vehicle to avoid rear-end collisions. And ACC provides assistance to the drivers in the task of longitudinal control during their motorway driving [3], [4].

The associate editor coordinating the review of this manuscript and approving it for publication was Bohui Wang.

With fast-developing communication technologies, cooperative ACC is very heated recently [5], [6]. It is appealing because of the enhancement of vehicle performance and situational awareness. However, cooperative ACC can be unreliable due to the immaturity of vehicle to vehicle communication [7]. Hence, ACC is still worth investigating.

A quantity of ACC car-following optimal control algorithms and strategies were proposed during the past decades. For example, two illustrious models, the optimal velocity model (OVM) [8] and intelligent driver model (IDM) [9], [10], initially designed to mimic human-driven vehicle's (HV) car-following behavior are then applied to describe ACC vehicle behavior. The OVM regulates the vehicle towards an optimal speed defined as a function of the time headway, however, it does not have a collision-free property. IDM addresses the safety problem by introducing extra parameters such as a brake term to constrain acceleration. Nevertheless, these models do not consider human driver

characteristics and have an obvious flaw in distinguishing the essential difference between HV's car-following and AV's car-following behavior.

Other than directly applying or modifying existed HV car-following models, a large amount of control theory based ACC algorithms are developed rapidly, which can be generally divided into three main categories: (i) optimal control with explicit objectives and hard constraints [11], [12], (ii) linear controllers [5], [13] and (iii) nonlinear controllers [14], [15]. The first type is usually implemented in a model predictive control (MPC) fashion [14], [16]–[20], which represents a series of control algorithms that use explicit process models to predict future responses of certain inputs. The MPC approach is attractive due to its flexibilities on objectives and constraints modelling. However, especially for constrained MPC, it does not guarantee feasible solutions and requires an efficient algorithm to solve the constrained optimization problem. Compared with MPC, objectives of unconstrained nonlinear and linear controllers are more fixed, and constraints are lack. Linear ACC controllers usually design the acceleration to be proportional to the spacing deviation and the relative speed with the predecessor, which are fast in computing and easier to apply in practice. Nonlinear controllers exist to depict some scenarios more precisely such as a mixed traffic environment consisting of AVs, HVs, and semi-autonomous vehicles while with the drawback of increasing calculation complexity [15]. In spite of the above-mentioned three categories of methods have both strengths and weaknesses, personalized preferences are barely considered in previous controller design. AVs are usually treated as simply homogenous.

Even though AV can satisfy the driving automation requirement, personalized automation such as some certain driving styles, driver-based preferences, and driver patterns has rarely been considered inside the ACC design yet. As far as authors know, current ACC control algorithms cannot really incorporate users driving preference [21]. Besides, as AV's market penetration grows gradually, the number of user-preferred settings can naturally diversify [22], [23]. Among all the personal settings, risk-taking preference, also known as risk-sensitivity, is an extremely important characteristic due to the fact that it has a close relationship with the safety of car-following behaviors and should be heterogeneous for different drivers depending on the states and current driving situations. Hence, it is necessary to fill the gap on risk-sensitive personalization interpreting in AV control to satisfied driver's expectation better.

Additionally, comfort in AV control process is also critical. To avoid sudden starts and stops, expensive control strategy [23] which has an extra penalty on large control input (acceleration) can also help to smooth car-following behaviors based on different drivers' preference. Hence, to increase the diversity of ACC controller behaviors, we present a personalized stochastic optimal control algorithm for AV. The developed ACC algorithm shed the light on diversifying drivers' choices to satisfy the personal requirements, which gives two detailed contributions: Firstly, to show the functionality of being personalized in risk-sensitive preference, the control framework applies linear exponential-of-quadratic Gaussian (LEQG) (or risk sensitive linear quadratic) mechanism via extending LQG, in which the cost function is designed as an exponential form and involves a risk-sensitive parameter to interpret different willingness degrees to bear additional risk under mixed uncertainties [25]–[28]. As a result, various driving trajectories and behaviors are generated by the controller based on different sensitive parameter settings. Secondly, control comfort requirement in the control process is also incorporated via the relative magnitude settings on weight matrices, i.e., switching between expensive control mode and non-expensive control mode. These contributions in ACC design are innovative and important to becoming practical functions in ACC future industrialization. For verification, the presented controller is evaluated through several simulation experiments. The results show that the proposed controller can provide effective and convergent control as well as generate different trajectories for AVs with different risk preferences. The control framework has overall satisfying performances.

The remainder of the paper is organized as follows: Section II presents the continuous and discretized system state-space formulation and introduces control design. Section III describes the validation process of the proposed control strategy. Finally, Section IV summarizes the key findings and provides future research direction.

II. STATE-SPACE FORMULATION AND CONTROL DESIGN

This section starts by presenting the system state-space formulations in both continuous and discretized form, then introduces the proposed LEQG stochastic optimal control problem. For simplicity, some preliminaries are stated firstly. We postulate that all ACC vehicles can receive real-time information (e.g. velocity, acceleration) detecting by the sensors regarding the direct predecessor. We also assume all discretized uncertainties are zero-mean additive white Gaussian noises. Besides, communication delay and vehicular actuation delay are not considered here since they are not large compared to the control sample period [5].

A. CONTINUOUS STATE-SPACE FORMULATION

Accordingly, this contribution applies the state-space formulation for ACC system propose by Zhou *et al.*, [18]. The notable constant time headway (CTH) policy is used in this paper, thus the target equilibrium spacing at time t is computed as below:

$$s^*(t) = v(t) \times t^* + s_0 \tag{1}$$

where $s^*(t)$ denotes the desired spacing at time t, $v(t)$ represents the speed of the follower, t^* is a predefined desired time gap and s_0 is the minimum spacing between two vehicles in standstill situation for safety concern. We then define:

$$\Delta v(t) = v^*(t) - v(t) \tag{2}$$

where $v^*(t)$ represents the velocity of the leader. $\Delta v(t)$ is the relative speed of an ACC vehicle (follower) with its leader.

Using the above-mentioned variables, the system state x can be naturally defined as follows:

$$x(t) = (s(t) - s^*(t), \Delta v(t))^T \tag{3}$$

where $s(t)$ is follower's actual relative spacing with the leading vehicle. The first term of $x(t)$ represents the deviation with the equilibrium spacing at time t. Thus, the above system can be formulated as a linear time invariant (LTI) system with system state $x(t)$ and control input $u(t)$ by assuming the leading vehicle follows a constant speed during each sampling interval, the state equation follows:

$$\dot{x}(t) = Ax(t) + Bu(t) + V(t) \tag{4}$$

$$A = \begin{pmatrix} 0 & 1 \\ 0 & 0 \end{pmatrix}, \quad B = \begin{pmatrix} -t^* \\ -1 \end{pmatrix} \tag{5}$$

where $u(t)$ is the acceleration of an ACC vehicle as well as the desired system input at time t, $V(t)$ refers to the exogenous system disturbance which consists of relative speed term and acceleration term due to unmodeled vehicular and aerodynamics factors. Eq. (4) and Eq. (5) are obtained according to definitions in Eqs. (1–3) and the physical relationship among the distance, velocity, and acceleration. Meanwhile, Eq. (4) depicts the correlation between the derivative of the system state, system state, control input and uncertainty.

B. STATE-SPACE FORMULATION DISCRETIZATION

Though continuous system is usually more desirable, in application, systems usually have a control frequency. Therefore, to be more realistic, we discretize the continuous ACC system proposed in Eq. (4) by assuming control input $u(t)$ to be zero-order hold same as Zhou *et al*. [18]:

$$x_{t+1} = A_d x_t + B_d u_t + V_t \tag{6}$$

where

$$A_d = e^{At_s} \tag{7}$$

$$B_d = (\int_0^{t_s} e^{A\tau} d\tau) B \tag{8}$$

$$x_0 = \mu_0 \tag{9}$$

Note that zero-order hold means that within each sampling interval, the control input is time-invariant [29]. t_s is the control frequency (interval) of the controller. x_t, u_t, V_t represents the discretized version of system state, control input and system error, respectively. The sequence V_t has zero mean and satisfies independent and identical distribution. Furthermore, V_t is independent of x_t. A_d and B_d are the discretized form for weight matrices which are calculated as Eq. (7) and Eq. (8) respectively. μ_0 is a predefined constant value, indicating the initial system state. After discretization, the system becomes more realistic and are available for digital-computer implementation.

C. STATE FEEDBACK CONTROL STRATEGY

Our designing of stochastic optimal longitudinal control of ACC system applies a linear exponential-of-quadratic Gaussian control framework. LEQG control problem, adopts risk sensitive control and differential game theory, is an important generalization of the linear-quadratic Gaussian (LQG) control problem. LEQG replaces the original quadratic cost function in LQG with an exponential form of a quadratic functional of the state and the input, hence, is called "LEQG". Furthermore, a risk-sensitive parameter is introduced in the cost function of LEQG. Other than being a part of the control framework, the parameter has a realistic meaning in this paper in depicting different levels of risk preference for AVs when facing oscillations.

Firstly, the state feedback control strategy is discussed, which is a widely applied technique for adaptive cruise controllers. In this strategy, the observation of system is assumed to be perfect. The control input is a linear function of the state that defined as state multiplies feedback gain. The running cost at each time point t of an ACC vehicle in the system is defined as:

$$\Upsilon_t = x_t' M_t x_t + u_t' N_t u_t \tag{10}$$

where x_t' denotes the transpose of matrix x_t, u_t' denotes the transpose of matrix u_t. The way of transpose expression is also suitable for other matrices in this paper. M_t and N_t are the predetermined weight matrices of state and input at time t respectively. In order to guarantee the non-negative, symmetry property and ensure Eq. (10) is always in a quadratic form, define the M_t and N_t in a diagonal form as below:

$$M_t = \begin{pmatrix} \beta_{1,t} & 0 \\ 0 & \beta_{2,t} \end{pmatrix}, \quad N_t = \omega_t \tag{11}$$

where $\beta_{1,t}, \beta_{2,t}, \omega_t > 0$ and all of them are predefined constant values addressing control target weights. The exponential form quadratic cost function J_θ of the system is then defined in Eq.(12) and Eq.(13) which subjects to the state space and initial constraints (Eq.(6), Eq.(9)) concurrently [26].

$$J_\theta(x_t, u_t) = 2\theta^{-1} \log E(e^{\frac{1}{2}\theta G}) \tag{12}$$

where

$$G = \sum_{t=1}^{T} \Upsilon_t \tag{13}$$

Note that E is the expectation operator. T is the study period. θ in Eq. (12) is a risk-sensitive parameter used to interpreting different extent responses of dynamic systems on exogenous risk.

The objective of the proposed ACC controller is to minimize the cost function defined by Eq. (12) and Eq. (13) which commits to regulating vehicle's velocity and spacing towards the equilibrium one in terms of running cost function, i.e., to do its best to remain the equilibrium state $x(t) = (0, 0)^T$. Hence, the optimal control input solution set of the system cost function constrained by Eq. (6) for ACC is defined by:

$$u^* = \arg\min \{J_\theta(x_t, u_t)\} \tag{14}$$

The value of θ has a significant meaning in LEQG problem and ACC control. The analysis of risk behaviors has been widely discussed in economics also known as risk evaluation, which aims to assess the willingness degree to bear additional risk. For a system optimizer of LEQG type, different signs of θ suggest different risk-sensitive attitudes, the magnitude of θ can represent the level of preference for each scenario. Hence, θ is critical in AV risk personalization. More explicitly, cases of $\theta = 0, \theta > 0$ and $\theta < 0$ respectively correspond to the situation of risk-neutral, risk-preferring and risk-averse attitude from an economist perspective [25]. The classification reason can be expressed as follow.

In the case $\theta > 0$, to minimize the cost function, the controller actually attempts to minimize the expectation of a convex increasing function defined in Eq. (12). The penalties of the occurrences of values that larger than $E(G)$ are treated overweight than those less than $E(G)$ to achieve system goal.

Whereas in the case $\theta < 0$, one is maximizing the expectation of a convex decreasing function in Eq. (12). The system will take an opposite evaluation in this situation which means to set the penalties of occurrences of values less than $E(G)$ larger than those greater than $E(G)$.

Particularly, the developed control problem will reduce to a conventional LQG problem when $\theta = 0$. And the cost function for LQG problem relaxes to:

$$J(x_t, u_t) = E(\sum_{t=1}^{T} x_t' M_t x_t + u_t' N_t u_t) = E(G) \quad (15)$$

Remark 1: According to [26], the sign of risk-sensitive parameter θ can also be interpreted from the perspective of deterministic linear quadratic differential game in which both control input and system disturbance are viewed as two players.

Scenario 1 ($\theta > 0$): Cooperative game. Player u_t assumes that player V_t will be cooperative in minimizing the cost function even though the preliminary for V_t is to satisfy the white Gaussian distribution. Then the cost function can be expressed as a cooperative deterministic game as below:

$$\underset{\{u_t\},\{v_t\}}{\text{minimize}} \sum_{t=1}^{T} (x_t' M_t x_t + u_t' N_t u_t + V_t' Q_t V_t) \quad (16)$$

subject to the constraints Eq. (6) and Eq. (9), where $Q_t^{-1} = E\left[V_t V_t'\right]; t = 0, \ldots, T, E[V_t] = 0, t = 0, \ldots, T$.

Scenario 2 ($\theta < 0$): Non-cooperative game. Player u_t assumes that player V_t will not cooperate and even mess up in minimizing the quadratic criterion, that is to say u_t treats the expectation of V_t to be max (despite the fact that V_t behaves as random Gaussian variable), then the cost function is expressed as follows:

$$\min_{\{u_t\}} \max_{\{v_t\}} \sum_{t=1}^{T} (x_t' M_t x_t + u_t' N_t u_t + V_t' Q_t V_t) \quad (17)$$

subject to Eq. (6) and Eq. (9).

Based on ***Remark 1***, we can have a more comprehensive understanding of the function of the risk-sensitive parameter in LEQG.

Correspondingly, when $\theta > 0$, the solutions of LEQG state feedback control problem defined before are equivalent to the solutions of the cooperative deterministic game defined by Eq. (6) and Eq. (16). With a risk-preferring attitude, the ACC controller is thought to be more optimistic than reality (best case design) as it views system disturbance as minimized.

When $\theta < 0$, similarly, the equivalent deterministic game problem is determined by Eq. (6) and Eq. (17) and viewed as a non-cooperative situation. With a risk-averse attitude, the ACC controller will be treated as more pessimistic than reality (worst case design) since it maximum the intensity of system noise.

For the LEQG state feedback control problem defined by Eq. (6), Eq. (12) and Eq. (13), the optimal control takes the form [25], [27]:

$$u_{\theta,t}^* = K_{\theta,t} x_t \quad (18)$$

where $K_{\theta,t}$ is known as the feedback gain calculated by:

$$K_{\theta,t} = -N_t^{-1} B_d' \times (B_d N_t^{-1} B_d' + \tilde{P}_{\theta,t+1}^{-1})^{-1} \times A_d \quad (19)$$

The negative sign in Eq. (19) is to indicate the negative feedback property. And $P_{\theta,t}$ is determined by solving the discrete-time algebraic Riccati equation (DARE):

$$P_{\theta,t} = M_t + A_d' \times (B_d N_t^{-1} B_d' + \tilde{P}_{\theta,t+1}^{-1})^{-1} \times A_d \quad (20)$$

$$\tilde{P}_{\theta,t+1} = (P_{\theta,t+1}^{-1} - \theta\xi)^{-1}, \quad t = 0, 1, \ldots, T-1 \quad (21)$$

ξ is defined as the variance matrix of system disturbance V_t. In this paper, the tilde operator, $\sim$, means an estimate of a variable.

D. OUTPUT FEEDBACK CONTROL STRATEGY

The precondition to applying the aforementioned state feedback control strategy is that to assume the system has perfect measurement. Nevertheless, it is highly unrealistic in practice due to inevitable measurement uncertainties. Here we introduce the measurement equation considering sensor disturbance as below:

$$y(t) = Cx(t) + W(t) \quad (22)$$

where

$$C = \begin{pmatrix} 1 & 0 \\ 0 & 1 \end{pmatrix} \quad (23)$$

Eq. (22) describes the measurement (observation) equality, in which $y(t)$ is the measurement detecting from AV's on-board sensor and $W(t)$ represents the sensor error (disturbance) at time t. C is the measurement matrix which is set to be a unit diagonal matrix without losing generality.

The covariance matrix of two disturbances $[V(t), W(t)]'$ are given by:

$$\Delta = \begin{pmatrix} \xi & \gamma \\ \gamma' & \Gamma \end{pmatrix} \quad (24)$$

with

$$\xi = H(t), \quad \Gamma = S(t), \quad \gamma = \text{cov}(V(t), W(t)) \quad (25)$$

where $H(t)$ and $S(t)$ are the variances for $V(t)$ and $W(t)$ respectively, γ is the covariance of $V(t)$ and $W(t)$.

Similarly, we discretize Eq. (22) using the same method mentioned before and we obtain:

$$y_t = C_d x_t + W_t \tag{26}$$

where C_d is the discretized form for C. W_t represents the discretized measurement error. H_t and S_t are the discretized expression for the covariance $H(t)$ and $S(t)$, computed as:

$$H_t = \int_0^{t_s} e^{A\tau} M(t) d\tau \tag{27}$$

$$S_t = \frac{t_s}{N(t)} \tag{28}$$

For the LEQG problem defined by Eq. (6), Eq. (12), Eq. (13) and Eq. (26), the output feedback case optimal control can be obtained by using the separation principle [30], which states that control and estimation are two independent processes in designing. Therefore, based on this principle, output feedback control is designed to remain the original control framework while replaces the unmeasurable parameter in the objective function to its estimated value. The detailed optimal solution follows:

$$u^*_{\theta,t} = K_{\theta,t}(I - \theta R_{\theta,t} P_{\theta,t})^{-1} \mu_{\theta,t} \tag{29}$$

Further, let $x_0 \sim N(\mu_0, R_0)$, where N represents the normal distribution. With the cost function defined in Eq. (12) and Eq. (13), the output feedback DARE has the form:

$$\begin{aligned} R_{\theta,t+1} = \xi + A_d \tilde{R}_{\theta,t+1} A_d' - (\gamma + A_d \tilde{R}_{\theta,t+1} C_d') \\ \times (\Gamma + C_d \tilde{R}_{\theta,t+1} C_d')^{-1} \times (\gamma + A_d \tilde{R}_{\theta,t+1} C_d')' \end{aligned} \tag{30}$$

where

$$\tilde{R}_{\theta,t} = (R_{\theta,t}^{-1} - \theta M_t)^{-1}; \quad t = 0, 1, \ldots, T-1, \; R_{\theta,0} = R_0 \tag{31}$$

For state estimation, the Kalman filter which contains prediction stage and update stage is applied [31]. We use superscripts $+$ and $-$ to denote predicted estimates and updated estimates, respectively. Firstly, the predicted state estimate $\mu^-_{\theta,t+1}$ at time $t+1$ is acquired from the previously updated state estimate $\tilde{\mu}^+_{\theta,t}$:

$$\tilde{\mu}^-_{\theta,t+1} = A_d \tilde{\mu}^+_{\theta,t} + B_d u_t \tag{32}$$

$$\tilde{\mu}^+_{\theta,t} = \tilde{R}_{\theta,t} \times R^{-1}_{\theta,t} \tilde{\mu}^-_{\theta,t} \tag{33}$$

Note that we tend to use a different symbol μ to distinguish the state in state feedback control and output feedback control.

In the update stage, the measurement residual $\tilde{z}_{t+1}$ which represents the difference between the true measurement and the estimated measurement is computed:

$$\tilde{z}_{t+1} = y_{t+1} - C_d \tilde{\mu}^-_{\theta,t+1} \tag{34}$$

The filter estimates the real measurement via using the product of the predicted state estimate and the discretized measurement matrix. And we then multiply the residual by the Kalman gain to update the state estimate together with the predicted state estimate:

$$\tilde{\mu}^+_{\theta,t+1} = \tilde{\mu}^-_{\theta,t+1} + L_{\theta,t+1} \tilde{z}_{t+1} \tag{35}$$

where $\tilde{\mu}^+_{\theta,t+1}$ is the current updated state estimate and the Kalman gain $L_{\theta,t+1}$ equals:

$$L_{\theta,t+1} = (\gamma' + C_d \tilde{R}_{\theta,t} A_d')' \times (\Gamma + C_d \tilde{R}_{\theta,t} C_d')^{-1} \tag{36}$$

where $K_{\theta,t}$ and $P_{\theta,t}$ have been defined in Eq. (19) and Eq. (20).

Noting that the output feedback strategy has the same logic with the state feedback strategy in understanding the functionality of θ. For brevity, detailed discussions are omitted here.

E. EXPENSIVE AND NON-EXPENSIVE CONTROL MODE

To be better personalized in control comfort requirements, two control modes are proposed below.

1) EXPENSIVE CONTROL MODE

Controlling of a time-invariant dynamic system with a heavy constraint on the input amplitudes is known as expensive control since the control cost of input u is more expensive relative to that of the state x [24]. To achieve this, set $N_t > M_t$ in the system to show the additional emphasis on smooth driving, indicating that the system gives priority to smaller control input in order to accelerate moderately in the study period.

2) NON-EXPENSIVE CONTROL MODE

When M_t and N_t defined in Eq. (10) are set to have same magnitudes of value or $N_t < M_t$, it is considered to be a non-expensive driving scenario. No extra attention is paid on the input term in non-expensive control mode.

Based on the methodology given above, except for the state feedback case and output feedback case, the proposed ACC framework can represent six different AV driving behaviors shown as Fig.1. In Fig.1, the first level branch is based on the system control mode and the second level branch distinguishes different categories of risk sensitivity. For example, risk-preferring driving behavior under expensive control mode implying the ACC controller has an optimistic driving attitude towards uncertainties meanwhile the acceleration

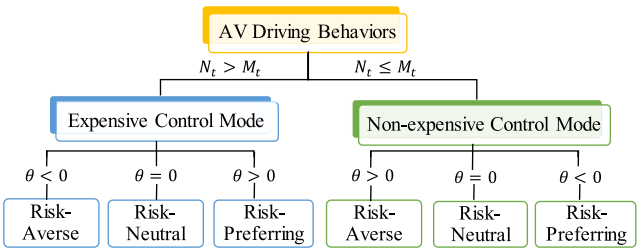

FIGURE 1. AV driving behaviors classification.

action magnitude is limited to some extent during the control period.

III. EXPERIMENTS AND RESULTS ANALYSIS

In order to validate the performance of the proposed stochastic linear optimal control method, numerical simulation experiments have been conducted since field test is expensive and beyond scope. This section includes four parts. We firstly begin with an experiment set-up part to initialize the condition and set some parameter default values in Section III.A. Based on that, we systematically designed multiple scenarios with different control parameters to show our proposed framework can produce the heterogeneous driving behaviors. Specifically, we conducted a sensitivity analysis to compare the performances difference between input feedback case and output feedback case with different risk sensitivity parameters in Section III.B. Then we analyzed heterogeneous driving behaviors caused by joint impact of risk sensitivity and magnitudes of disturbances in Section III.C. Finally, two different control modes adopting output feedback strategy with varied values of risk sensitivity are discussed in Section III.D.

A. EXPERIMENT SET-UP

As mentioned before, we consider simulation experiments to validate the proposed algorithm. Firstly, Table 1 gives the default values of corresponding parameters. The simulation study period T is set as $5s$. Considering the balance of controller efficiency and proper driving comfort, we set $\beta_{1,t} = \beta_{2,t} = 1$ and $\omega_t = 1$ as default values firstly. Giving the same weights to the deviation from the equilibrium spacing and speed with the preceding vehicle suggests the equal significance of collision avoidance and driving smoothness. Besides, through parameter tuning, the values of the risk parameter θ in the proposed controller choose –0.2, 0 and 0.2 for risk-averse ($\theta < 0$), risk-neutral ($\theta = 0$) and risk-preferring ($\theta > 0$) case respectively. As for the system initial condition, the initial state is set to be $x_0 = (2, 0)^T$ as an illustration for the following experiments, meaning that the start spacing deviation of system to be $2m$ and the start speed difference with the predecessor to be $0m/s$. Note that without additional expression, controller parameters comply with default values.

TABLE 1. Parameters.

Parameters	Default value
$\beta_{1,t}$	1
$\beta_{2,t}$	1
ω_t	1
$t_s(s)$	0.1
$T(s)$	5
$t^*(s)$	1
γ	0
θ	-0.2,0,0.2

B. STATE FEEDBACK STRATEGY AND OUTPUT FEEDBACK STRATEGY PERFORMANCE COMPARISON UNDER SAME INTENSITIES OF MIXED UNCERTAINTIES

We firstly conducted a sensitivity analysis on the control performance comparison between the output feedback case and state feedback case with varied variances of both system disturbance and measurement disturbance to investigate joint impact caused by the risk preference and disturbance intensities on control performance. The test range of measurement disturbance is set according to the authoritative report National Highway Traffic Safety Administration [32], which states that radar's range of accuracy for distance and velocity are $\pm 0.3m$ and $\pm 0.83m/s$. Therefore, based on the reference value and considering control range feasibility, we vary the variance of measurement disturbance S_t from 0 to 0.2 with an increment of 0.05. The units for distance and speed are m and m/s, respectively. As for the variance of system disturbance, no relative reference was found. Hence, we also vary H_t from 0 to 0.2 with an increment of 0.05 to guarantee that H_t is consistent with the magnitude of S_t. For simplicity, we postulate that measurement disturbance and system disturbance are non-correlative as it has been shown that the potential correlation between them does not have a critical impact (i.e., $\gamma = 0$).

The relative change percentage of the total cost is chosen to be an indicator to compare the performance with/without considering measurement noises, which is calculated as follows:

$$\text{Relative change percentage} = \frac{J_{\theta,State} - J_{\theta,Output}}{J_{\theta,Output}} \times 100\% \tag{37}$$

where $J_{\theta,State}$ and $J_{\theta,Output}$ represent the total control cost for the state feedback case and output feedback case under same mixed uncertainties respectively. We set $J_{\theta,Output}$ as a reference here. The results with different risk sensitive parameters are given in Fig. 2. To thoroughly describe the sensitivity analysis results, we discuss them from three aspects. (i) No measurement disturbance ($y = 0$). In this case, with available system states and perfect measurement, the relative change percentages stay zero. (ii) Small measurement disturbance ($y = 0.05$). In this situation, the indicator value of risk-averse case ($\theta = -0.2$) reaches the maximum values compared with other measurement disturbance intensity settings, changing from 1.8% to 4.1% as the system disturbance variance increases. For risk-neutral case ($\theta = 0$), the relative change percentages locate in 2.5% to 5.1%. The indicator values of risk-preferring case ($\theta = 0.2$) range from 3.3% to 5.9%. (iii) Large measurement disturbance ($y = 0.2$). We find conspicuous differences exist in terms of indicator among scenarios with different risk parameters: risk-preferring case acquires the largest indicator value while risk-averse case has nearly zero relative change percentage, risk-neutral case is slightly less than the maximum indicator value. Hence, the above indicates that the proposed controller can generate different trajectories for different risk-resistance settings to depict human drivers' risk preference in AV control.

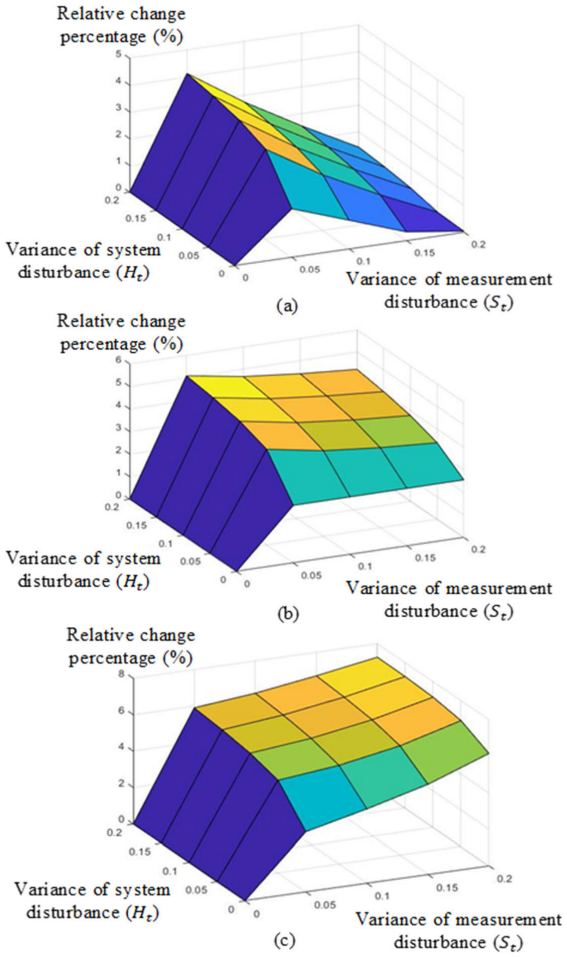

FIGURE 2. Sensitivity analysis of disturbances: (a) $\theta = -0.2$; (b) $\theta = 0$ (c) $\theta = 0.2$.

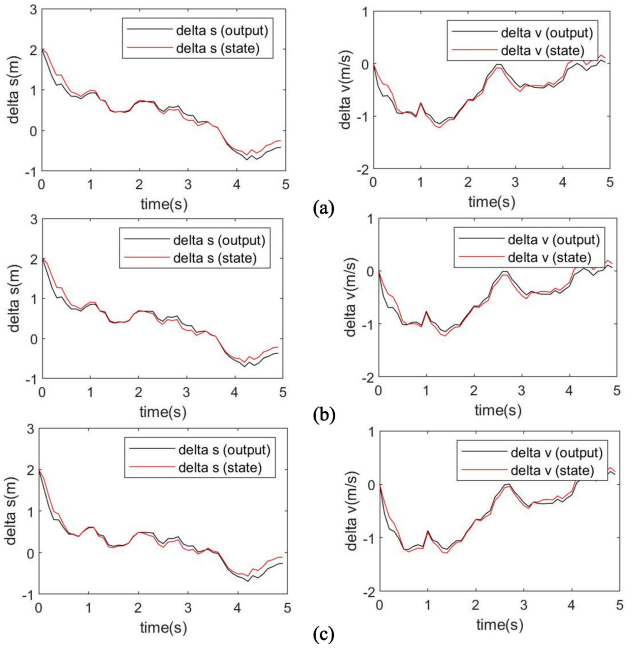

FIGURE 3. Performance comparison for state feedback case and output feedback case ($H_t = 0.2, S_t = 0.05$): (a) $\theta = -0.2$; (b) $\theta = 0$ (c) $\theta = 0.2$.

To further validate this, we plot the vehicle's state evolutions shown as Fig.3. Besides, an observe suggests that output feedback case always outperforms than state feedback case because the relative change percentage is always positive within the experiment region.

C. HETEROGENEOUS DRIVING BEHAVIOR CAUSED BY JOINT IMPACT OF RISK SENSITIVITY AND MAGNITUDES OF DISTURBANCES

Since the behaviors of different risk sensitivity will react heterogeneously under different magnitudes of disturbances, here we investigate the heterogeneous driving behavior caused by joint impact induced by different risk sensitivity and magnitudes of disturbances. Since the experiments of previous part have verified that output feedback case outperforms state feedback case, we will no longer discuss the latter one in the following experiments. Further, we extend the behavior analysis using the default value given in Table 1 but varying the system disturbance H_t varies in Table 1 but varying the system disturbance H_t varies from $0 \times I^{2\times 2}$ to $0.2 \times I^{2\times 2}$ with 0.1 increment to evaluate the magnitude θ. The measurement disturbance variance is set at 0.1. The results are shown in Fig. 4. Furthermore, Fig.5 gives the cost distribution of three discriminated values of θ corresponds to the two stochastic cases in Fig.4, in which the total cost is computed as the sum of state deviation cost and control input cost.

$$C_{\theta,\text{State deviation}} = \sum_{t=1}^{T} x_{t,\theta} x'_{t,\theta} \tag{38}$$

$$C_{\theta,\text{Control input}} = \sum_{t=1}^{T} u_{t,\theta} u'_{t,\theta} \tag{39}$$

where $C_{\theta,\text{State deviation}}$ is the state deviation cost and $C_{\theta,\text{Control input}}$ is the control input cost. $x_{t,\theta}$ and $u_{t,\theta}$ are state and input considering risk sensitive parameter.

Fig. 4 has the characteristics that the system states converge from the initial condition to the equilibrium state $(0, 0)^T$ for all cases within the study period. We can also find that when no system disturbance exists, i.e., the deterministic scenario, state recovery evolution exhibits as a regular smooth process. With the growth of H_t, more fluctuations manifest for both state and speed deviations during convergence. Meanwhile, if we fix the intensity of system disturbance and observe vertically, the optimistic case ($\theta = 0.2$) performs obviously different from the other two cases in stochastic situations. Therefore, the above proves that for the developed control algorithm, both risk sensitivity and magnitudes of disturbance have a significant function in generating heterogeneous driving behaviors. Notice that $\theta = \pm 0.2$ does not have a symmetric influence on control performance (see Fig.4), we repute this is owing to the exponential

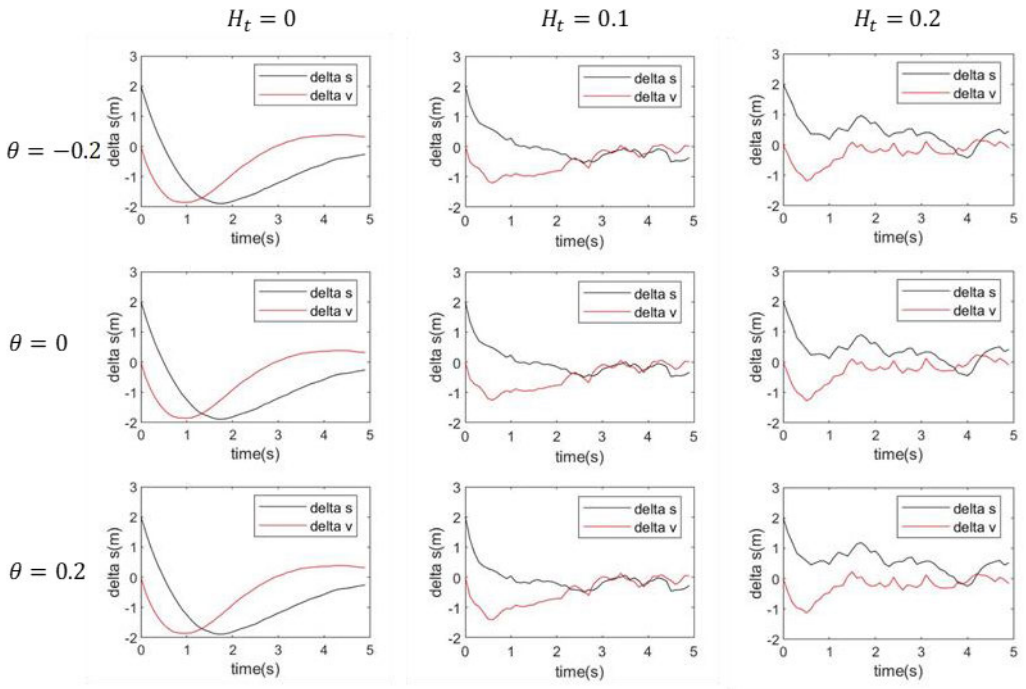

FIGURE 4. Performance analysis for joint impact of risk sensitivity and magnitudes of system disturbances.

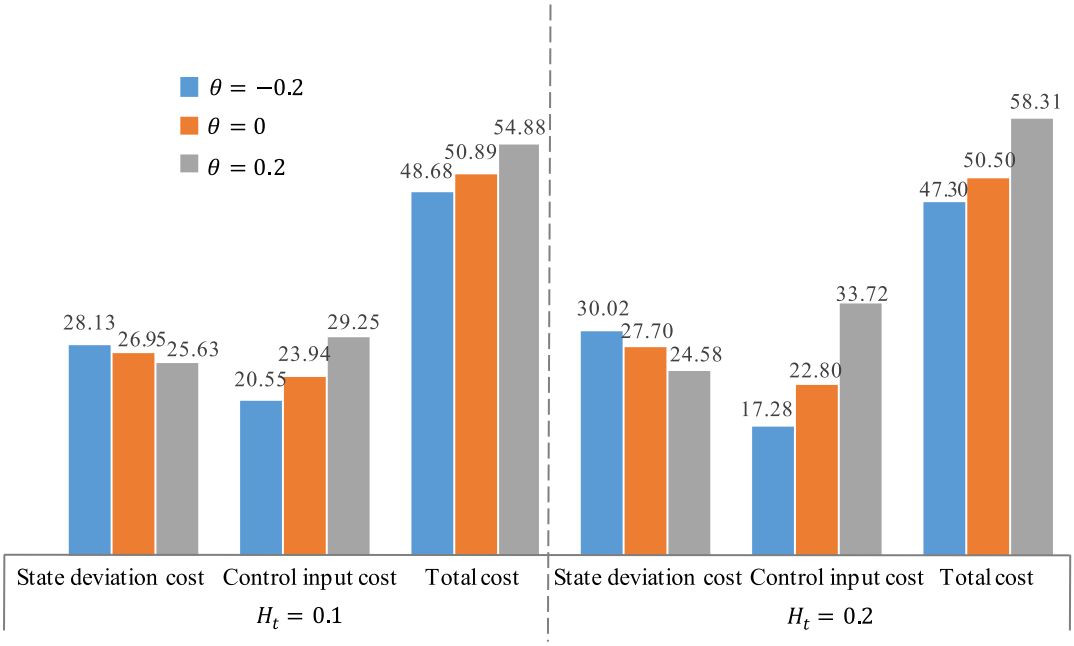

FIGURE 5. AV's cost distribution of different system disturbances.

design on control cost function instead of the traditional linear one.

Therefore, for a more in-depth analysis, we study the asymmetric controller response to θ. This time we fix H_t as $0.2 \times I^{2\times 2}$ for three cases while setting $\theta = -2$ for the risk-averse case. The results are provided in Fig.6. From Fig.6, the distinctions in control evolution can be obviously seen among three circumstances. Similarly, Fig.7. provides the explicit cost distribution. In terms of the total cost, risk-averse case ($\theta = -2$) costs most followed by risk-neutral case ($\theta = 0$) and risk-preferring case ($\theta = 0.2$). The underlying reason may be that risk-averse case viewed system disturbance as maximum, therefore, more system cost is demanded against the disturbance. Further, with the changing of risk sensitivity

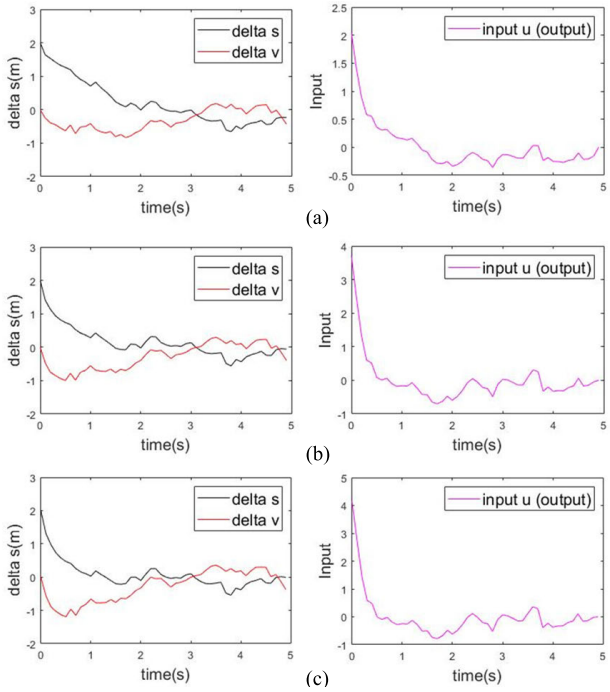

FIGURE 6. Asymmetric controller response to the risk-sensitive parameter: (a) $\theta = -0.2$; (b) $\theta = 0$ (c) $\theta = 0.2$.

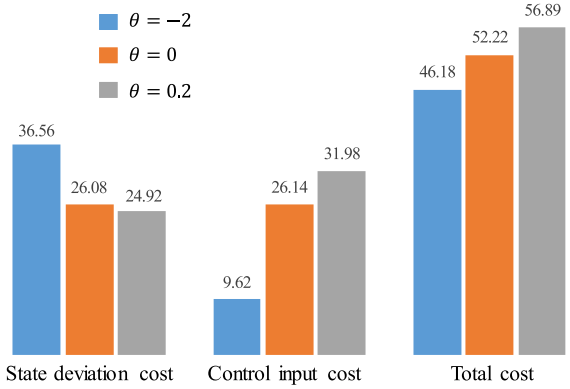

FIGURE 7. AV's cost distribution of asymmetric controller response.

parameter, state deviation cost and control input cost seem to have an opposite developing trend in relative magnitude order.

D. HETEROGENEOUS DRIVING BEHAVIOR CAUSED BY JOINT IMPACT OF RISK SENSITIVITY AND EXPENSIVE/NON-EXPENSIVE CONTROL MODE

Expensive control mode and non-expensive control mode are realized by changing the values of predetermined weight matrices M_t and N_t. As for the expensive control mode, to avoid sudden starts and stops, we set $M_t \times N_t^{-1} = \frac{1}{2} \times I^{2\times 2}$ such that the variation of input is paid additional attention. On the other hand, we set $M_t \times N_t^{-1} = 2 \times I^{2\times 2}$ to represent non-expensive control which puts more emphasis

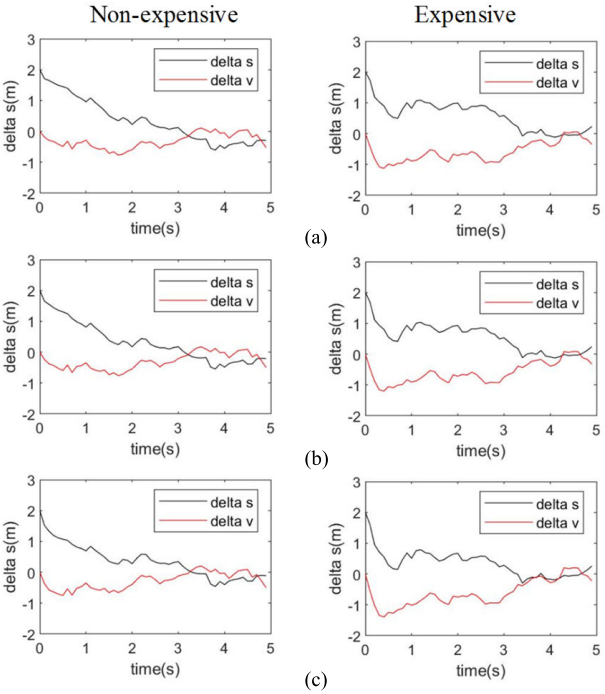

FIGURE 8. Performance comparison for non-expensive and expensive control mode with different risk sensitive parameters: (a) $\theta = -0.2$; (b) $\theta = 0$ (c) $\theta = 0.2$.

on state deviation. H_t, S_t are predefined as fixed values 0.1 and 0.2 respectively here. The results are reported in Fig. 8.

Compare horizontally, the spacing convergence speed towards the equilibrium one for non-expensive control mode is quicker than expensive mode. Meanwhile, the relative speed error fluctuates in a smaller range for non-expensive mode compared with the expensive mode.

This is mainly because the corresponding selectable range of acceleration for expensive control mode shrinks due to the larger input weight matrix setting and objective of minimizing the cost function. Hence, the system approaches equilibrium state slower meanwhile less speed change rate causes speed oscillations more difficult to recover. Studying vertically gives us more insights into the impacts of the risk parameters on system control smoothness after convergence. The best smoothness performance happens in the risk-preferring case ($\theta = 0.2$). The reason can be derived as risk-preferring attitude considers minimized disturbance during driving, therefore have a smoother driving pace under less disturbance.

IV. CONCLUSION

Diverse driving preference requirements on risk call for the designing of personalized ACC controller considering various human drivers' risk sensitivities. In this paper, a driving risk-resistance characteristic depicting optimal control algorithm for ACC is presented based on the LEQG control framework. The proposed algorithm can qualify and quantify AV's risk sensitivity preference description under

mixed disturbances as well as incorporating driving comfort. With different settings of risk-sensitive parameters and control modes, six categories of AVs' heterogeneous driving behaviors when facing disturbances can be interpreted. For the validation of this contribution, sensitivity analysis and several tests are accomplished. Generally, the control performances of the proposed algorithm are satisfying. According to the results of simulated experiments, risk sensitivity, disturbance magnitude, and control mode are all effective factors on trajectory generation. Future work will extended current framework to CACC case by allowing cooperation multiple vehicles (such as [33]–[35]).

REFERENCES

[1] J. VanderWerf, S. Shladover, N. Kourjanskaia, M. Miller, and H. Krishnan, "Modeling effects of driver control assistance systems on traffic," *Transp. Res. Rec.*, vol. 1748, no. 1, pp. 167–174, 2001.

[2] A. Vahidi and A. Eskandarian, "Research advances in intelligent collision avoidance and adaptive cruise control," *IEEE Trans. Intell. Transp. Syst.*, vol. 4, no. 3, pp. 143–153, Sep. 2003.

[3] G. Marsden, M. McDonald, and M. Brackstone, "Towards an understanding of adaptive cruise control," *Transp. Res. C, Emerg. Technol.*, vol. 9, no. 1, pp. 33–51, Feb. 2001.

[4] A. Kesting, M. Treiber, M. Schönhof, and D. Helbing, "Adaptive cruise control design for active congestion avoidance," *Transp. Res. C, Emerg. Technol.*, vol. 16, no. 6, pp. 668–683, Dec. 2008.

[5] Y. Zhou, S. Ahn, M. Wang, and S. Hoogendoorn, "Stabilizing mixed vehicular platoons with connected automated vehicles: An H-infinity approach," *Transp. Res. B, Methodol.*, vol. 132, pp. 152–170, Feb. 2020.

[6] S. Gong, J. Shen, and L. Du, "Constrained optimization and distributed computation based car following control of a connected and autonomous vehicle platoon," *Transp. Res. B, Methodol.*, vol. 94, pp. 314–334, Dec. 2016.

[7] C. Wang, S. Gong, A. Zhou, T. Li, and S. Peeta, "Cooperative adaptive cruise control for connected autonomous vehicles by factoring communication-related constraints," *Transp. Res. C, Emerg. Technol.*, vol. 113, pp. 124–145, Apr. 2020.

[8] M. Bando, K. Hasebe, K. Nakanishi, and A. Nakayama, "Analysis of optimal velocity model with explicit delay," *Phys. Rev. E, Stat. Phys. Plasmas Fluids Relat. Interdiscip. Top.*, vol. 58, no. 5, pp. 5429–5435, Nov. 1998.

[9] A. Kesting and M. Treiber, "Calibrating car-following models by using trajectory data: Methodological study," *Transp. Res. Rec., J. Transp. Res. Board*, vol. 2088, no. 1, pp. 148–156, Jan. 2008.

[10] A. Kesting, M. Treiber, and D. Helbing, "Enhanced intelligent driver model to access the impact of driving strategies on traffic capacity," *Phil. Trans. Roy. Soc. A, Math., Phys. Eng. Sci.*, vol. 368, no. 1928, pp. 4585–4605, Oct. 2010.

[11] S. Hoogendoorn, R. Hoogendoorn, M. Wang, and W. Daamen, "Modeling driver, driver support, and cooperative systems with dynamic optimal control," *Transp. Res. Rec., J. Transp. Res. Board*, vol. 2316, no. 1, pp. 20–30, Jan. 2012.

[12] Y. Wei, C. Avcı, J. Liu, B. Belezamo, N. Aydın, P. Li, and X. Zhou, "Dynamic programming-based multi-vehicle longitudinal trajectory optimization with simplified car following models," *Transp. Res. B, Methodol.*, vol. 106, pp. 102–129, Dec. 2017.

[13] Y. Zhou and S. Ahn, "Robust local and string stability for a decentralized car following control strategy for connected automated vehicles," *Transp. Res. B, Methodol.*, vol. 125, pp. 175–196, Jul. 2019.

[14] M. Vajedi and N. L. Azad, "Ecological adaptive cruise controller for plug-in hybrid electric vehicles using nonlinear model predictive control," *IEEE Trans. Intell. Transp. Syst.*, vol. 17, no. 1, pp. 113–122, Jan. 2016.

[15] L. Zhang and G. Orosz, "Consensus and disturbance attenuation in multi-agent chains with nonlinear control and time delays," *Int. J. Robust Nonlinear Control*, vol. 27, no. 5, pp. 781–803, Mar. 2017.

[16] G. Gunter, C. Janssen, W. Barbour, R. E. Stern, and D. B. Work, "Model-based string stability of adaptive cruise control systems using field data," *IEEE Trans. Intell. Vehicles*, vol. 5, no. 1, pp. 90–99, Mar. 2020.

[17] M. Wang, S. P. Hoogendoorn, W. Daamen, B. van Arem, B. Shyrokau, and R. Happee, "Delay-compensating strategy to enhance string stability of adaptive cruise controlled vehicles," *Transportmetrica B, Transp. Dyn.*, vol. 6, no. 3, pp. 211–229, Jul. 2018.

[18] Y. Zhou, S. Ahn, M. Chitturi, and D. A. Noyce, "Rolling horizon stochastic optimal control strategy for ACC and CACC under uncertainty," *Transp. Res. C, Emerg. Technol.*, vol. 83, pp. 61–76, Oct. 2017.

[19] Y. Zhou, M. Wang, and S. Ahn, "Distributed model predictive control approach for cooperative car-following with guaranteed local and string stability," *Transp. Res. B, Methodol.*, vol. 128, pp. 69–86, Oct. 2019.

[20] S. Zhao and K. Zhang, "A distributionally robust stochastic optimization-based model predictive control with distributionally robust chance constraints for cooperative adaptive cruise control under uncertain traffic conditions," *Transp. Res. B, Methodol.*, vol. 138, pp. 144–178, Aug. 2020.

[21] A. Rosenfeld, Z. Bareket, C. V. Goldman, D. J. LeBlanc, and O. Tsimhoni, "Learning drivers' behavior to improve adaptive cruise control," *J. Intell. Transp. Syst.*, vol. 19, no. 1, pp. 18–31, Jan. 2015.

[22] P. Fancher, Z. Bareket, and R. Ervin, "Human-centered design of an Acc-with-braking and forward-crash-warning system," *Veh. Syst. Dyn.*, vol. 36, nos. 2–3, pp. 203–223, 2001.

[23] A. HasanzadeZonuzy, S. Arefizadeh, A. Talebpour, S. Shakkottai, and S. Darbha, "Collaborative platooning of automated vehicles using variable time-gaps," in *Proc. Annu. Amer. Control Conf. (ACC)*, Jun. 2018, pp. 6715–6722.

[24] A. Pearson, "Linear optimal control systems," *IEEE Trans. Autom. Control*, vol. AC-19, no. 5, pp. 631–632, Oct. 1974.

[25] P. Whittle, "Risk-sensitive linear/quadratic/Gaussian control," *Adv. Appl. Probab.*, vol. 13, no. 4, pp. 764–777, Dec. 1981.

[26] D. Jacobson, "Optimal stochastic linear systems with exponential performance criteria and their relation to deterministic differential games," *IEEE Trans. Autom. Control*, vol. AC-18, no. 2, pp. 124–131, Apr. 1973.

[27] A. J. Shaiju and I. R. Petersen, "Formulas for discrete time LQR, LQG, LEQG and minimax LQG optimal control problems," *IFAC Proc. Volumes*, vol. 41, no. 2, pp. 8773–8778, 2008.

[28] T. E. Duncan, "Linear exponential quadratic stochastic differential games," *IEEE Trans. Autom. Control*, vol. 61, no. 9, pp. 2550–2552, Sep. 2016.

[29] C. Chen, *Linear System Theory and Design*, vol. 22, no. 3. New York, NY, USA: Oxford Univ. Press, 1998.

[30] T. T. Georgiou and A. Lindquist, "The separation principle in stochastic control, redux," *IEEE Trans. Autom. Control*, vol. 58, no. 10, pp. 2481–2494, Oct. 2013.

[31] Y. Kim and H. Bang, "Introduction to Kalman filter and its applications," in *Introduction to Kalman Filter and Its Applications*. London, U.K.: IntechOpen, 2018, pp. 1–16.

[32] *LIDAR Speed-Measuring Device Performance Specifications (Report No. DOT HS 809 811)*, NHTSA, Washington, DC, USA, 2013.

[33] B. Wang, W. Chen, and B. Zhang, "Semi-global robust tracking consensus for multi-agent uncertain systems with input saturation via metamorphic low-gain feedback," *Automatica*, vol. 103, pp. 363–373, May 2019.

[34] F. Gao, X. Hu, S. E. Li, K. Li, and Q. Sun, "Distributed adaptive sliding mode control of vehicular platoon with uncertain interaction topology," *IEEE Trans. Ind. Electron.*, vol. 65, no. 8, pp. 6352–6361, Aug. 2018.

[35] B. Wang, W. Chen, J. Wang, B. Zhang, and P. Shi, "Semi-global tracking cooperative control for multi-agent systems with input saturation: A multiple saturation levels framework," *IEEE Trans. Autom. Control*, early access, May 6, 2020, doi: 10.1109/TAC.2020.2991695.

JIWAN JIANG received the B.S. degree from Southwest Jiaotong University, Chengdu, China, in 2018. She is currently pursuing the master's degree with the School of Transportation, Southeast University, China.

She has been a Visiting Research Scholar with the Department of Civil and Environmental Engineering, University of Wisconsin–Madison, USA, since 2019. Her principal research areas include the longitudinal control of connected and automated vehicles and mixed vehicle platoon control.

FAN DING received the B.S. degree in information from Southeast University, Nanjing, China, in 2012, and the M.S. degree in computer science and the Ph.D. degree in civil engineering from the University of Wisconsin–Madison, in 2016 and 2017, respectively. He is currently an Assistant Professor with the Joint Research Institute on Internet of Mobility, Southeast University, and the University of Wisconsin–Madison. His research interests include intelligent transportation systems (ITSs), mobile traffic sensor modeling, proactive traffic management, and transportation big data analytics.

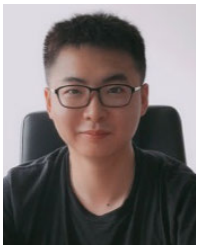

YANG ZHOU received the M.S. degree in civil and environmental engineering from the University of Illinois at Urbana–Champaign, Champaign, IL, USA, in 2015, and the Ph.D. degree in civil and environmental engineering from the University of Wisconsin–Madison, Madison, WI, USA, in 2019. He is currently a Postdoctoral Researcher of civil engineering from the University of Wisconsin–Madison. His main research interests include connected automated vehicles robust control, interconnected system stability analysis, traffic big data analysis, and microscopic traffic flow modeling.

JIAMING WU received the B.S. and M.S. degrees from the School of Transportation Science and Engineering, Harbin Institute of Technology, in 2014, and the Ph.D. degree from Southeast University, in 2019. He is currently a Postdoctoral Researcher with the Department of Electrical Engineering, Chalmers University of Technology, Gothenburg, Sweden. His research interests include connected and automated vehicles platoon control, signalized intersection design, and performance analysis.

HUACHUN TAN (Member, IEEE) received the Ph.D. degree in electrical engineering from Tsinghua University, Beijing, China, in 2006. He used to be an Associate Professor with the School of Mechanical Engineering, Beijing Institute of Technology, Beijing, from September 2009 to June 2018. He is currently a Professor with the School of Transportation, Southeast University, Nanjing, China. His research interests include image engineering, pattern recognition, and intelligent transportation systems.